JOURNAL OF SOLID STATE CHEMISTRY 33, 413–419 (1980)

The Structure of Orthorhombic $Na_2Ti_9O_{19}$, a Unit-Cell Twinning of Monoclinic $Na_2Ti_9O_{19}$, Determined by 1-MV High-Resolution Electron Microscopy

YOSHIO BANDO, MAMORU WATANABE, AND YOSHIZO SEKIKAWA

National Institute for Researches in Inorganic Materials, Sakura-mura, Niihari-gun, Ibaraki 300-31, Japan

Received July 11, 1979; in revised form October 10, 1979

The crystal structure of the orthorhombic disodium nonatitanate, $Na_2Ti_9O_{19}$, has been determined on the basis of 1-MV high-resolution structure images, in which each site of the titanium and sodium atoms is clearly resolved. The crystal has an orthorhombic symmetry with lattice parameters $a = 12.2$, $b = 3.78$, and $c = 30.1$ Å. The space group of the crystal is either *Ccmm* or *Cc2m*. The crystal structure of the orthorhombic nonatitanate is closely related to that of the monoclinic nonatitanate reported previously in which the structure contains sodium titanium dioxide bronze-type units connected by bridging TiO_6 octahedra. The orthorhombic crystal can be described in terms of a unit-cell twinning of the monoclinic crystal. It is shown that migrations of sodium ions occur by electron beam irradiation.

Introduction

The sodium titanate is represented by a composition series $Na_2O \cdot nTiO_2$ ($n \geq 1$). The crystal structures of $Na_2Ti_3O_7$ ($n = 3$), $Na_2Ti_6O_{13}$ ($n = 6$), and $Na_2Ti_7O_{15}$ ($n = 7$) were determined by Andersson and Wadsley (*1, 2*) and Wadsley and Mumme (*3*). They clarified the relationships between the crystal structures and chemical compositions. The sodium tetratitanate, $Na_2Ti_4O_9$($n = 4$), was found by Dion *et al.* (*4*) to be isostructural with $Tl_2Ti_4O_9$. Andersson and Wadsley (*5*) determined the crystal structure of sodium titanium dioxide bronze, $Na_xTi_4O_8$ (x, approximately 0.8), and showed that the crystal had a framework different from those of sodium titanates. Meanwhile, the crystals of tri- and hexatitanates were known to form easily. Sodium titanates with $n > 7$, however, had never been reported until recently the authors (*6*) found a new compound, the monoclinic disodium nonatitanate, $Na_2Ti_9O_{19}$ ($n = 9$), prepared by hydrothermal reactions. Because the products consisted of small fibrous crystals, it was difficult to determine its crystal structure by a single-crystal X-ray diffraction method.

The 1-MV high-resolution electron microscope (Hitachi 1250 kV) constructed in our institute is very powerful for determination of frameworks of unknown crystal structures, because it can resolve nearly 2.0 Å at an accelerating voltage of 1 MV with axial illumination and using a goniometer stage (*7*). The technique for the structure anlysis by 1-MV high-resolution electron microscopy has been applied to some inorganic compounds and the structures of $Bi_7Ti_4NbO_{21}$ (*8*), $Bi_2W_2O_9$ (*9*), $TiS_{1.46}$ (*10*), and $Yb_3Fe_4O_{10}$ (*11*) have been determined

0022-4596/80/090413-07$02.00/0

from finely resolved structure images taken along two or more directions, in which each of the cation sites was resolved. By using this technique, the authors (*12*) tried to determine the crystal structure of the monoclinic $Na_2Ti_9O_{19}$. Figure 1 shows a structure image taken along the *b* axis from a very thin part of the crystal region. The nonatitanate has a monoclinic symmetry with lattice parameters $a = 12.2$ Å, $b = 3.78$ Å, $c = 15.3$ Å, and $\beta = 98°$. The 1-MV structure image showed that each site of the titanium and sodium atoms was resolved as dark dots and white spots, respectively. The crystal structure obtained from the image is shown in the inset. The monoclinic sodium titanate has a framework different from those of tri-, hexa-, and heptatitanates. The structure consists of TiO_6 octahedra and enclosed sodium ions, forming the framework of the sodium titanium dioxide bronze-type units, which is indicated as symbols *DD* in the figure. The bronze-type units are connected by bridging TiO_6 octahedra, the rows of which are indicated as *B*. The structure is represented by a sheet sequence of . . . *BDDB* . . . along the *c* axis at intervals of 15.3 Å.

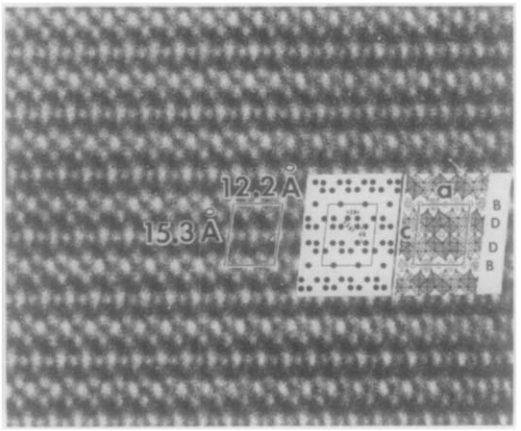

FIG. 1. The structure image of the monoclinic $Na_2Ti_9O_{19}$, observed prevously (*12*) under the 1-MV high-resolution electron microscope. The incident electron beam is parallel to the [010] direction. Two types of sheets with dark and gray dots are indicated as *D* and *B*, respectively. The image contrast consists of the sheet sequence of . . . *BDDB* . . . along the *c* axis at intervals of 15.3 Å. The schematic representation of titanium atoms is shown by solid circles in the inset, in which the separations of two adjoining dark dots are indciated. The structure model is inserted into the figure. The heavy squares indicate TiO_6 octahedra at $y = 0$, and the light squares those at $y = \frac{1}{2}$. The dashed squares show bridging octahedra at $y = \frac{1}{4}$ and $\frac{3}{4}$. The open circles show sodium ions. The unit cell is outlined: $a = 12.2$ Å, $b = 3.78$ Å, $c = 15.3$ Å, and $\beta = 98°$.

Recently, we have found orthorhombic $Na_2Ti_9O_{19}$ crystals, prepared by hydrothermal reactions. The crystals formed consisted of small fibers, the appearance of which was quite similar to that of the monoclinic crystal. It was therefore difficult to analyze its crystal structure by the X-ray method.

In this study, the crystal structure of the orthorhombic disodium nonatitanate, $Na_2Ti_9O_{19}$, has been determined on the basis of 1-MV high-resolution electron microscopy. It was shown that the image contrast of the orthorhombic crystal was closely related to that of the monoclinic crystal and the crystal structure of the orthorhombic nonatitanate could be described in terms of the unit-cell level twinning or polysynthetic twinning of the monoclinic nonatitanate. It was also found that migrations of sodium ions occur by electron beam irradiation.

Experimental

A new compound of the orthorhombic $Na_2Ti_9O_{19}$ was prepared by hydrothermal reactions. The procedure for preparing the crystals was similar to that for the monoclinic nonatitanate previously reported (*6*). The X-ray amorphous titanium dioxide gel and sodium hydroxide solution were enclosed in a platinum capsule. The capsule was placed in a Tuttle cold-test tube laid horizontal. The high-temperature zone was kept at 550°C and the growth zone at 410°C. The pressure was kept at 10^3 atm. The

duration of the reaction was about 1 month. The crystals obtained were slightly bluish. The products consisted of fibrous crystals which were thinner than a few micrometers in size.

The chemical composition was determined by electron probe microanalysis. The molar ratio of Ti to Na was estimated to be 4.5 ± 0.05. The density of the specimen was measured to be 3.67 ± 0.04, which was the same as that obtained for the monoclinic crystal.

The fibrous crystals were picked from the aggregates and crushed in an agate mortar to fragments of several hundred angstroms. They were placed on a holey carbon supporting film and observed under the 1-MV electron microscope. The accelerating voltage was operated at 1 MV. The astigmatism of the objective lens was corrected by directly observing the granular images of the carbon supporting films. The objective aperture size used corresponded to about 0.5 $Å^{-1}$ in reciprocal space. The image contrast obtained at underfocus values between 500 and 1000 Å was interpreted intuitively. The direct magnification was 2.5×10^5 times and the exposure time was about 3 sec.

Results and Interpretation

Many electron diffraction patterns corresponding to various reciprocal lattice sections were taken from $Na_2Ti_9O_{19}$ crystal fragments. Two of them are shown in Fig. 2. The crystal symmetry is orthorhombic with lattice parameters $a = 12.2$, $b = 3.78$, and $c = 30.1$ Å, where they are refined by X-ray powder diffraction. In order to obtain true extinction rules from electron diffraction patterns, the specimens were tilted so that the only $00l$ reflections were excited, where double diffraction was not geometrically produced. Then, the systematic absent reflections were hkl with $h + k = 2n + 1$ and $0kl$ with $k = l = 2n + 1$, $h0l$ with $h = 2n + 1$, $hk0$ with h + $k = 2n +$

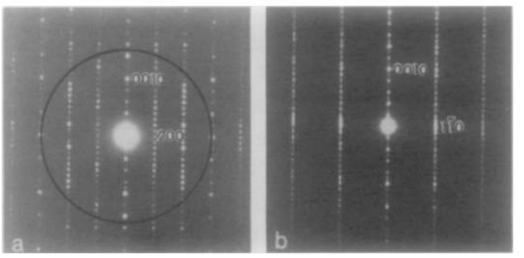

FIG. 2. Electron diffraction patterns from *O*-$Na_2Ti_9O_{19}$ crystal fragments, taken under the 1-MV electron microscope. The incident electron beam is parallel to the (a) [010] and (b) [110] directions. The size and the position of the objective aperture is outlined.

1. The possible space groups are therefore $Cc2m$ (noncentrosymmetric) and $Ccmm$ (centrosymmetric). The length of the c axis for the orthorhombic crystal (*O*-$Na_2Ti_9O_{19}$) is $2c_m \cdot \sin \beta$, where c_m and β denote the lattice parameters of the monoclinic crystal (*M*-$Na_2Ti_9O_{19}$). The crystallographic data for *O*-$Na_2Ti_9O_{19}$ are shown in Table I.

Figure 3 shows a structure image of *O*-$Na_2Ti_9O_{19}$, taken from the very thin part of the crystal region. The incident electron beam was parallel to the [010] direction. The corresponding diffraction pattern is shown in Fig. 2a, in which the size and the position of the objective aperture are out-

TABLE I

CRYSTALLOGRAPHIC DATA FOR ORTHORHOMBIC $Na_2Ti_9O_{19}$

Symmetry	Orthorhombic
Unit-cell dimensions	a = 12.2 Å b = 3.78 Å c = 30.1 Å
Systematic absent reflections	hkl with $h + k = 2n + 1$ $0kl$ with $k = l = 2n + 1$ $h0l$ with $h = 2n + 1$ $hk0$ with $h + k = 2n + 1$
Possible space groups	$Cc2m$ and $Ccmm$
D(cal) = 3.74 g · cm^{-3} D(obs) = 3.67 g · cm^{-3} Z = 4	

lined. About 110 waves were used for imaging. The image contrast was constructed by the sheets with dark and gray dots which alternated along the c axis. In the previous observation of some oxides (*9, 11*), it is shown that each site of heavy cation atoms could be imaged as a dark or a gray dot. By this analogy, in the present case the dark and gray dots were assigned as the sites of titanium atoms. The arrangements of titanium atoms are shown schematically by solid circles in the inset. The sheets with dark dots are named D and $\bar{D}$, where $\bar{D}$ is derived by rotating D for 180° about the b axis. On the other hand, the sheets with gray dots are named B. The present crystal structure can be represented by a stacking sequence of the sheets of . . . $DB\bar{D}\bar{D}BD$ . . . along the c axis at intervals of 30.1 Å. The separation distances of two adjoining titanium atoms within the sheets D (or $\bar{D}$) are either 2 or 3 Å, while those between the neighboring sheets D (or $\bar{D}$) are about 4 Å. The separations were the same as those found in M-$Na_2Ti_9O_{19}$, in which observed separations of the titanium atoms could be accounted for by analogy with known structures of sodium titanates and sodium titanium dioxide bronze. Thus the interpretation of the structure image was carried out in the same manner as in the previous work (*12*). The structure model obtained on the basis of the interpretation of the structure image appears as an inset in the picture.

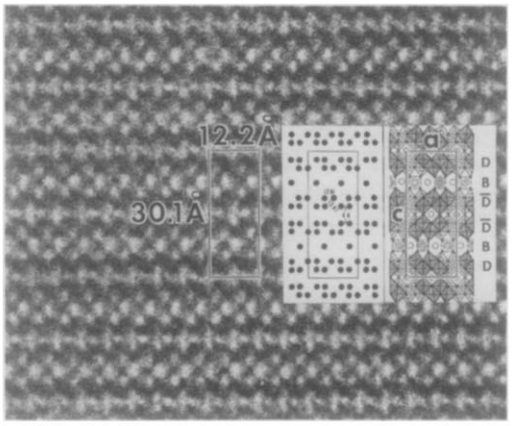

FIG. 3. A structure image of O-$Na_2Ti_9O_{19}$ crystal, taken under the 1-MV high-resolution electron microscope. The incident electron beam is parallel to the [010] direction and the corresponding diffraction pattern is shown in Fig. 2a. The image contrast is closely related to that of Fig. 1. The sheets with dark dots are indicated as D and $\bar{D}$, where $\bar{D}$ is obtained by rotating D for 180° about the b axis. The sheets with gray dots are indicated as B. The image contrast consists of the sheet sequence of . . . $DB\bar{D}\bar{D}BD$ . . . along the c axis at intervals of 30.1 Å. The schematic representation of titanium atoms is shown by solid circles. The structure model is shown in the inset, in which the symbols have the same meanings as those in Fig. 1.

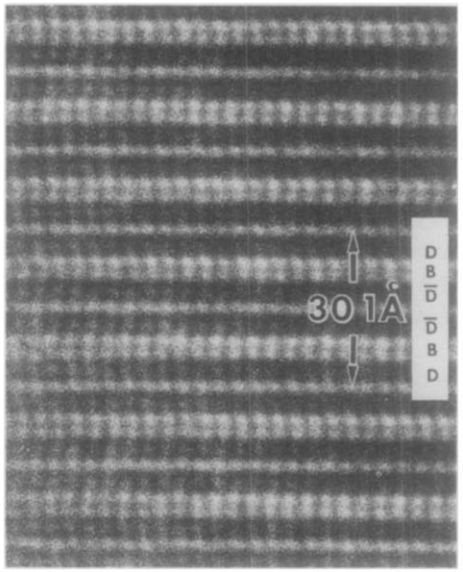

FIG. 4. A structure image of O-$Na_2Ti_9O_{19}$ crystal, taken with the incident electron beam parallel to the [110] direction. The corresponding diffraction pattern is shown in Fig. 2b. The structure is constructed by the sheet sequence of . . . $DB\bar{D}\bar{D}BD$ . . . along the c axis at intervals of 30.1 Å.

Figure 4 shows a structure image taken with the incident electron beam parallel to the [110] direction. The corresponding diffraction pattern is shown in Fig. 2b. In this projection, dark dots were more clearly resolved than those in Fig. 3, because the separations between the dark dots perpendicular to the c axis were as large as 3.8 Å.

The dark dots corresponded to the sites of titanium atoms also in the projection and they arrayed in zigzag chains along the c axis at intervals of 30.1 Å. The contrast of the dark dots in the sheets B was half as strong as that in the sheets D (or $\bar{D}$). This means that the numbers of titanium atoms in the sheets B projected onto the (110) plane are half as large as that in the sheets D (or $\bar{D}$). The image contrast thus interpreted in Fig. 4 corresponds well to the inset model of Fig. 3.

In the proposed crystal structure of O-$Na_2Ti_9O_{19}$ projected onto the (010) plane which is illutrated in the inset in Fig. 3 and also in Fig. 5c, squares denote TiO_6 octahedra and open circles sodium ions. The arrangement of oxygen atoms is speculated from the observation of titanium atoms. The positions of sodium ions are designated on the basis of the crystal chemical consideration to follow. As seen in illustration, the structure contains two kinds of large holes and also two kinds of small holes. The former are large square- and hexagonal-shaped holes as viewed along the b axis, which are located between the sheets D (or $\bar{D}$) or in the sheets B, respectively. They seem to be large enough to accommodate sodium ions. On the other hand, the latter are small square- and trigonal-shaped holes, which are located between the sheets D (or $\bar{D}$) or in the sheets B, respectively. They are too small to accommodate sodium ions. It may therefore be reasonable to assume that the positions of sodium ions are within these large holes. The chemical composition of the present crystal requires that these large holes be occupied fully by sodium ions. The arrangement of the white spots corresponds well to those of all holes.

The space group of the present crystal is possibly related to the y positions of sodium ions. Because of the difficulty of obtaining structure images projected along the a axis or the c axis, where the presence of the mirror symmetry perpendicular to the b axis could be judged directly, the space group of the present crystal could not be determined uniquely.

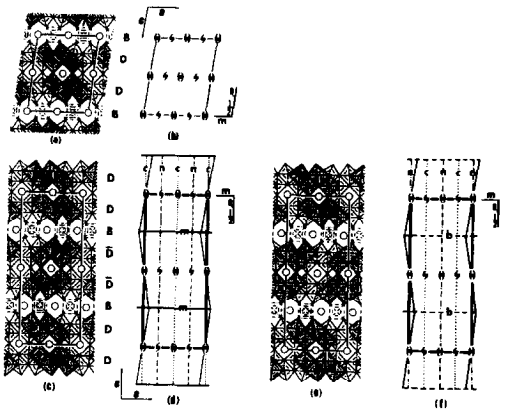

FIG. 5. The structure relations between M- and O-$Na_2Ti_9O_{19}$. (a) and (c) show crystal structures of M-$Na_2Ti_9O_{19}$ and O-$Na_2Ti_9O_{19}$ projected onto the (010) plane, respectively. (b) and (d) show symmetry elements for M-$Na_2Ti_9O_{19}$ and O-$Na_2Ti_9O_{19}$, respectively, in which the symbols have the same meanings as those used in the International Tables for X-Ray Crystallography. (e) and (f) show another model and its symmetry elements, respectively.

Discussion

1. Structural Relations between M-$Na_2Ti_9O_{19}$ and O-$Na_2Ti_9O_{19}$

The structures of M-$Na_2Ti_9O_{19}$ and O-$Na_2Ti_9O_{19}$ are extremely similar. Figures 5a and c show crystal structures of M-$Na_2Ti_9O_{19}$ and O-$Na_2Ti_9O_{19}$ projected onto the (010) plane, respectively. Both structures contain TiO_6 octahedra and enclosed sodium ions. Each octahedron shares an edge with another at the same level, forming a group of four interlinked TiO_6 octahedra. Each group is connected by the edge-sharing scheme to another which sits at a different level along the b axis, to form a sheet. Two sheets thus formed are linked to each other by the corner-sharing scheme to form a double sheet DD. This double sheet is identical to the framework of the sodium

titanium dioxide bronze, $Na_xTi_4O_8$, which was determined by Andersson and Wadsley (*5*). The structure of the sodium titanium dioxide bronze consists of infinite *DD* sheets. In sodium nonatitanates, the bronze-type units are connected by bridging TiO_6 octahedra. The structure of *M*-$Na_2Ti_9O_{19}$ has an ordered stacking sequence of . . . *BDDB* . . . along the *c* axis. The repeating period along the *c* axis is 15.3 Å. On the other hand, the stacking sequence in *O*-$Na_2Ti_9O_{19}$ is represented by . . . *BDD̄DBD* . . . , the period of which along the *c* axis is 30.1 Å. Since $\bar{D}$ means a sheet obtained by rotating the sheet *D* for 180° about the *b* axis, the bronze-type units *DD* and $D\bar{D}$ are in twin relation to each other. The twin plane is (001) and the twin boundaries are located at the sheets *B*. Thus, the structure of *O*-$Na_2Ti_9O_{19}$ can be described in terms of a unit-cell level twinning or polysynthetic twinning of *M*-$Na_2Ti_9O_{19}$. The structure relations between them are shown in Figs. 5b and d, in which symmetry elements are indicated. The elements are shown in terms of centrosymmetrical space groups. The orthorhombic cell is formed by the twin operation of the (001) mirror symmetry for the monoclinic cell, where symmetry elements of the monoclinic cell are preserved. It is possible to construct another model in terms of the unit-cell twinning as shown in Fig. 5e, where the model seems to correspond to the structure image in Fig. 3. In this model, the orthorhombic cell is constructed by operating the monoclinic cell by the *b* glide element perpendicular to the *c* axis (Fig. 5f). This model, however, does satisfy the result of electron diffraction patterns, because the model belongs to the space group of either *Cc2a* (noncentrosymmetrical) or *Ccmb* (centrosymmetrical).

It is interesting to note that TiO_6 octahedra bridging the bronze-type units are characteristic in sodium nonatitanate, for their edges are not shared by other octahedra. The titanium atoms of these bridging octahedra are located at the positions $y = \frac{1}{4}$ or $\frac{3}{4}$ in *M*-$Na_2Ti_9O_{19}$, and at the positions $y = 0$ or $\frac{1}{2}$ in *O*-$Na_2Ti_9O_{19}$. Therefore, it is speculated that the distortion due to such octahedra in *M*-$Na_2Ti_9O_{19}$ is larger than that in *O*-$Na_2Ti_9O_{19}$. But the distortion can only be determined accurately by the X-ray refinement of the crystal structure and a further discussion should await its result.

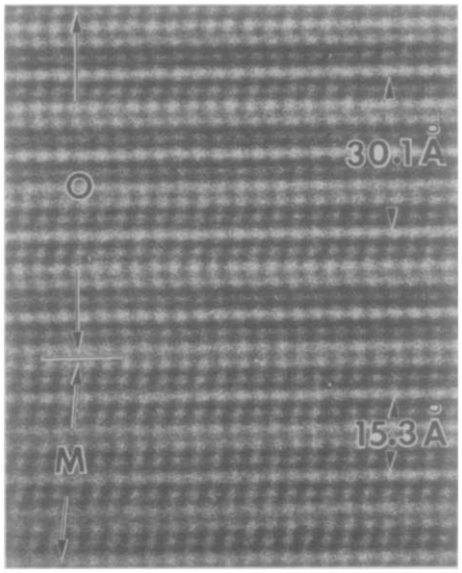

FIG. 6. An intergrowth of *M*-$Na_2Ti_9O_{19}$ crystal into the matrix of *O*-$Na_2Ti_9O_{19}$ crystal. The regions marked *M* and *O* correspond to the monoclinic and orthorhombic crystals, respectively.

From the structural similarities between *M*- and *O*-$Na_2Ti_9O_{19}$ discussed above, it is expected that an intergrowth between them occurs in a microsyntactic fashion. An example is shown in Fig. 6. In this picture, the regions marked *M* and *O* correspond to *M*-$Na_2Ti_9O_{19}$ and *O*-$Na_2Ti_9O_{19}$, respectively. The studied crystals often contained regions intergrown at a scale of a few tens of angstroms which corresponded to the streaks along the *c* axis present in Fig. 2b.

2. *Migrations of Sodium Ions Caused by Electron Beam Irradiation*

With a higher electron beam intensity,

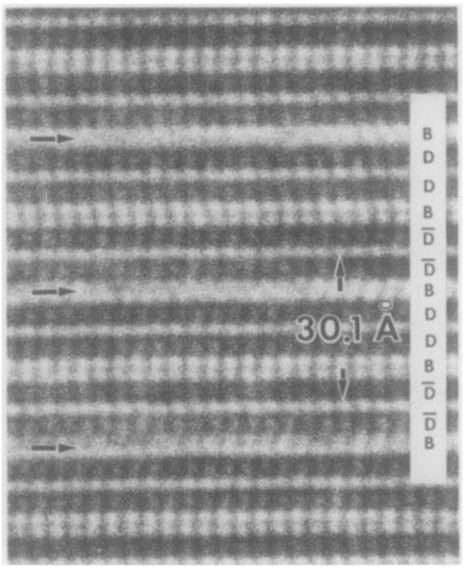

FIG. 7. Migrations of sodium ions caused by electron beam irradiation. The image contrast of the white spots marked by arrows is diffuse. The anomalies are formed in the regions of the sheets *B*.

the crystal often suffered from irradiation damage especially in the thin region. The result is shown in Fig. 7, where the projection is the same as that in Figs 4 and 6. In the regions marked by arrows, the image contrast of the white spots was diffuse. These anomalies of the image contrast were observed in the regions of the sheets *B*. This phenomenon is closely related to migrations of sodium ions caused by higher electron beam irradiation. As shown in Fig. 5c, the crystal contains two sites for sodium ions. One of them is located at the hexagonal-shaped holes and sodium ions in this site seem to be more loosely bonded by oxygen atoms than those located in the other site of large square-shaped holes, because the size of the former is as large as 4 Å while the size of the latter is as small as 3 Å. This suggests that sodium ions in the hexagonal-shaped holes easily migrate into the holes along the *b* axis after electron beam irradiation, resulting in the formation of the anomalies of the image contrast. Similar phenomena were observed by Matsui and Horiuchi (*13*), who found in an ionic conductor of β''-alumina that sodium ions migrate within the conduction plane.

Acknowledgments

The authors would like to express their deep gratitude to Dr. S. Kimura for valuable discussions and correcting the manuscript. They thank Drs. N. Nakazawa, F. Okamura, and S. Horiuchi and Mr. Y. Matsui for valuable discussions.

References

1. S. ANDERSSON AND A. D. WADSLEY, *Acta Crystallogr.* **14,** 1245 (1961).
2. S. ANDERSSON AND A. D. WADSLEY, *Acta Crystallogr.* **15,** 194 (1962).
3. A. D. WADSLEY AND W. G. MUMME, *Acta Crystallogr. Sect. B* **24,** 392 (1968).
4. M. DION, Y. PIFFARD, AND M. TOURNOUX, *J. Inorg. Nucl. Chem.* **40,** 917 (1978).
5. S. ANDERSSON AND A. D. WADSLEY, *Acta Crystallogr.* **15,** 201 (1962).
6. M. WATANABE, Y. BANDO, AND M. TSUTSUMI, *J. Solid State Chem.* **28,** 397 (1979).
7. S. HORIUCHI, Y. MATSUI, AND Y. BANDO, *Japan. J. Appl. Phys.* **15,** 2483 (1976).
8. S. HORIUCHI, T. KIKUCHI, AND M. GOTO, *Acta Crystallogr. Sect. A* **33,** 701 (1977).
9. Y. BANDO, A. WATANABE, Y. SEKIKAWA, M. GOTO, AND S. HORIUCHI, *Acta Crystallogr. Sect. A* **35,** 142 (1979).
10. Y. BANDO, M. SAEKI, Y. SEKIKAWA, Y. MATSUI, S. HORIUCHI, AND M. NAKAHIRA, *Acta Crystallogr. Sect. A* **35,** 564 (1979).
11. Y. MATSUI, K. KATO, N. KIMIZUKA, AND S. HORIUCHI, *Acta Crystallogr. Sect. B* **35,** 561 (1979).
12. Y. BANDO, M. WATANABE, AND Y. SEKIKAWA, *Acta Crystallogr. Sect. B* **35,** 1541 (1979).
13. Y. MATSUI AND S. HORIUCHI, *in* "Proceedings, Fifth International Conference on High Voltage Electron Microscopy, Kyoto," p. 321 (1977).